Discoloration of Aqueous Direct Blue 71 Solutions using UV/H$_2$O$_2$/Nano-SiO$_2$ Process

Maleki, A.[1], Nasseri, S.[2], Hadi, M.[2] and Solaimany Aminabad, M.[1*]

[1]Kurdistan Environmental Health Research Center, Faculty of Health, Kurdistan University of Medical Sciences, Sanandaj, Iran

[2]Center for Water Quality Research (CWQR), Institute for Environmental Research (IER), Tehran University of Medical Sciences, Tehran, Iran

ABSTRACT: The photolytic capability of SiO$_2$ nanoparticles (SiO$_2$-NP) for the discoloration of Direct Blue 71 as an environmentally pollutant dye via UV irradiation in the presence of H$_2$O$_2$ was assessed and optimized using response surface methodology (RSM) with a D-optimal design. The response of DB71 degradation was found to be sensitive to the independent factors of reaction time, SiO$_2$-NP and H$_2$O$_2$ concentrations. The discoloration process was not pH-dependent and the pH was not a significant factor in DB71 discoloration model. The approach provided statistically significant quadratic models, which were adequate to predict responses and to carry out optimization under the conditions studied. The maximum value of discoloration under the optimum operating conditions was determined to be 99.03% with a time of 16 min of irradiation and concentrations of 220 and 155 mg/L for H$_2$O$_2$ and SiO$_2$-NP respectively. The results showed that the discoloration increased about 11% by increasing SiO$_2$-NP concentration from 10 to 155 mg/L. The possible mechanism of SiO$_2$-NP catalytic performance was assessed. The kinetic study was also examined and indicated that the degradation of DB71 dye obeys Langmuir-Hinshelwood model.

Key words: Discoloration, Surface Response, Photocatalysis, SiO$_2$ Nanoparticle, Direct Blue

INTRODUCTION

There are many processes to remove dyes from colored effluents, some of which are applied in industry. These include adsorption process (Hadi *et al.*, 2011; McKay *et al.*, 2011; Hadi *et al.*, 2012; McKay *et al.*, 2014), biological processes (Taha *et al.*, 2014), chemical coagulation and precipitation (Saitoh *et al.*, 2014), nanofiltration (Yu *et al.*, 2012) and electro-coagulation & flotation (Zodi *et al.*, 2013). However, these conventional methods mainly remove the contaminants from wastewater and transfer them to solid wastes. Therefore, these physical, chemical and biological methods may not be sufficient in an appropriate manner for the removal of colored organic compounds. Among the other methods assessed for dyes removal, advanced oxidation processes (AOPs) under certain conditions can be very useful in removing colored compounds (Aquino *et al.*, 2013; Ibrahim *et al.*, 2013; Fernades Rêgo *et al.*, 2014). AOPs generate the highly reactive hydroxyl radical ($^\bullet$OH) to degrade recalcitrant chemicals present in wastewater.

Production of environment friendly end-products is one of the special main characteristics of these processes (Muruganandham & Swaminathan, 2006). In recent years, AOPs in wastewater treatment have been studied carefully and one of the most important AOP processes is heterogeneous AOP based on the use of ultraviolet light and semiconductors such as Au-TiO$_2$ catalyst (Zhang, 2012), ZnS nanoparticles (Tolia *et al.*, 2012), W/WO$_3$/TiO$_2$ bicomposite (Fraga *et al.*, 2013) and Ni/TiO$_2$ catalyst (Colpini *et al.*). In some other heterogeneous AOP processes the materials such ZnO (Zhai *et al.*, 2010), TiO$_2$ (Dong *et al.*, 2012) and Fe$_2$O$_3$-TiO$_2$-Ag (Cui *et al.*, 2013) were used as semiconductors with silica (SiO$_2$) as support material. Silica is basically inert for many reactions, but it shows noticeable activities towards some catalytic reactions (Fornasari & Trifirò, 1998). Silica was proven to remote photo-catalytic reactions, e.g. photo-catalytic degradation of methyl red by silica nanoparticles doped with Ag$^+$ or Au^{3+} (Badr *et al.*, 2008), methyl orange by gold silver

*Corresponding author E-mail: mehri.solaimany@yahoo.com

nano-core-silica nano-shell (Badr & Mahmoud, 2007), rhodamine B by silicon nanowires under UV and visible lights (Megouda *et al.*, 2011), photo-degradation of methyl orange by hybrid silica particles and TiO_2 core-shell microspheres (Shen *et al.*, 2011) and so on. According to above, the research groups have mainly investigated the effect of the silica combined with other materials in photo-catalytic process and there was seldom attention paid to the pure effect of silica nanoparticles (SiO_2-NPs) on photo-catalytic process, especially in the presence of hydrogen peroxide and UV light. Thus, this study was undertaken to clarifying SiO_2-NPs photo-catalytic ability in a combination process of UV-H_2O_2-SiO_2-NP for the discoloration of the dye solution. The SiO_2-NPs can be photoexcited under UV light below<"390 nm, which corresponds to a charge transfer from bonding orbital of Si-O to 2p non-bonding orbital of non-bridging oxygen (Skuja, 2000). In the present work, the photo-catalytic effect of SiO_2-NPs in an irradiation photo-catalytic process (UV intensity from 28 to 167 $\mu W/cm^2$) was studied for the discolorationof Direct Blue 71 (DB71) solution. The influencing factors investigated were the H_2O_2 and SiO_2-NP initial concentrations, initial pH of the solution, and the irradiation time duration. In this study, Response Surface Methodology (RSM) was used for optimizing the process by monitoring the solution final pH, TDS, EC, and temperature as the process responses. RSM method has been successfully applied for the optimization of processes for the pollutants removal from aqueous solutions (Kumar & Singh, 2014; Satapathy & Das, 2014). The kinetic experiments were also conducted with different values of H_2O_2 and SiO_2-NP to describe photo-catalytic degradation of the dye.

MATERIAL & METHODS

DB71 dye ($C_{40}H_{28}N_7NaO_{13}S_4$) with purity of >80% was purchased from Alvan sabet Co. in the west

if Iran (Hamadan) and used as such. The chemical structure of DB71 is shown in Fig.1. The maximum absorbance wavelength (λ_{max}) of DB71 was found to be 587 nm. Amorphous silicon oxide nanoparticles (SiO_2-NP) with >99% purity, particle size 10 nm, specific surface area 600 m^2/g, bulk density <0.10 g/cm^3 and true density 2.4 g/cm^3 were purchased from Nano Pars Lima Co. Ltd. in Tehran.

To prepare a stock solution of 10000 mg/L of H_2O_2, 26.81 cc of commercial solution (w/w: 33%) was diluted to 1000 cc. Hydrogen peroxide was obtained from Merck. The system as shown in Fig.2 included one germicidal lamp (Philips55 watt UV-C). During the bench-scale tests, all experiments were conducted at room temperature (20±2°C). UV process was operated using a low-pressure 55W mercury lamp (UV wavelength: 254 nm, length of the lamp: 909 mm, diameter of the lamp: 26 mm) placed inside a steel reactor. The effective volume of the reactor was 2.5 L. A double set of experiments were conducted to evaluate removal efficiency of DB71 dye. The UV fluence of 50000 $\mu Ws/cm^2$was evaluated for the all samples. Exposure times varied between 5 and 30 min. H_2O_2 dosages of 10 to 300mg/L were applied 30 s prior to UV radiation.
The absorbance values of DB71 solution before and after reaction were determined by the UV/Vis spectrophotometer at 587 nm. The discoloration rate of DB71 was calculated as below:

$$Decoloration(\%) = \frac{A_0 - A}{A} \times 100 \quad (1)$$

where A_0 and A are the measured absorbance values before and after irradiation, respectively.

In this study, the photo-catalytic discoloration of DB71 dye via UV irradiation in the presence of H_2O_2 and SiO_2-NP was optimized using RSM by utilizing Design-Expert 7.1. The runs were designed in accordance with D-optimal design and carried out
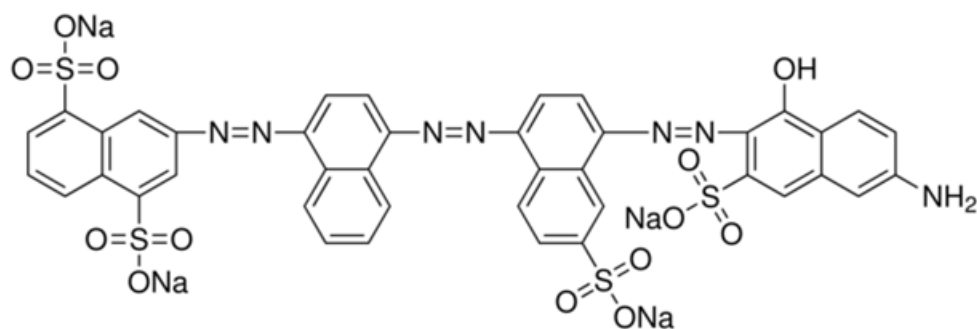
Fig. 1. Chemical structure of DB71
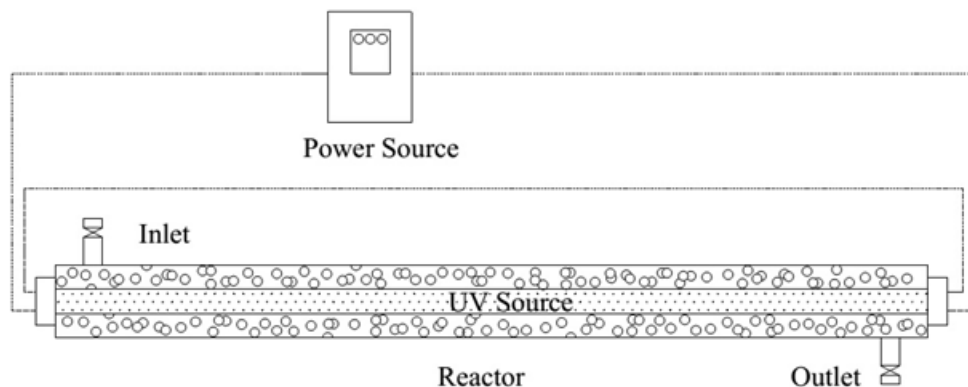
Fig. 2. Experiment setup for UV-based process

batch-wise. The D-optimal criterion can be used to select points for a mixture design in a constrained region. This criterion selects design points from a list of candidate points so that the variances of the model regression coefficients are minimized (Myers *et al.*, 2009). One of aims was to find a suitable approximating function in order to determine the dye removal efficiency and to investigate the operating conditions in a region for the factors at a certain operating specifications.

The independent variables of pH, reaction time, SiO_2-NP and H_2O_2 concentrations were coded with low (-1) and high (+1) levels in a D-optimal design as shown in Table 1. The test solution for the first run in Table 2, for example, was made by pouring 970 cc distilled water into a one liter beaker. Then 10 milligrams of SiO_2-NP were added to the beaker and the container was placed on a magnetic stirrer and stirred for 5 minutes. A little amount of the solution was taken and used as zero control for reducing the interference effect of nanoparticles on color measurement. Thereafter an appropriate amount of dye (50 mg) was added and pH was brought to 3. Then a volume of 30 ml H_2O_2 stock solution was added and the solution stirred for 30 second. One sample was taken after stirring the solution and the initial dye concentration spectrophotometrically (UV/Vis PG T80 Spectrophotometer), pH and temperature (Jenway 3510), TDS and EC (Jenway 4510) were

measured and recorded. The solution was poured into the UV reactor and exposed to UV light for 26.25 min. Thereafter the residual dye concentration and solution characteristics (pH, EC, TDS and temperature) were measured and recorded again. NaOH (0.10 mol/L) and H_2SO_4 (0.10 mol/L) were used to adjust the pH value of experimental solutions. Distilled water was used throughout this study and the experiments were carried out at room temperature.

Discoloration percent of DB71 dye (Y_1), final solution temperature (Y_2), final pH (Y_3), final electrical conductivity (Y_4) and the final total dissolved solids (Y_5) were the responses or dependent variables (Table 3).

The D-optimal designed experiments were improved with two replications in order to assess and reduce errors and were carried in randomized order. The response variables are related using the linear and quadratic relationships to the independent variables. A quadratic model, which also includes the linear model, is given as:

$$\eta = \beta_o + \sum_{j=1}^{k} \beta_j x_j + \sum_{j=1}^{k} \beta_{jj} x_j^2 + \sum_{i<j}\sum_{j=2}^{k} \beta_{ij} x_i x_j + \varepsilon_i \quad (2)$$

where η is the response, x_i and x_j are variables, k is the number of independent variables (factors), β_0 is the constant coefficient, βj, βjj and βij are interaction coefficients of linear, quadratic and the second-order

Table 1. Experimental design of photolytic degradation of DB71 dye

Factor	Name	Units	-1 Actual	+1 Actual	Mean	Std. Dev.
A	H_2O_2	mg/L	10	300	153.21	116.99
B	pH	-	3	9	6.03	2.59
C	SiO_2-NP	mg/L	10	300	161.53	127.69
D	Time	min	5	30	16.97	10.78

Table 2. Design matrix and observed values of the D-Optimal design

| Run | A:H_2O_2 | B:pH | C:SiO_2-NP | D:Time | Absorbance | |
					A_0	A
1	300.00	3.00	10.00	26.25	0.7630	0.0050
2	300.00	3.00	300.00	5.00	0.8440	0.2350
3	10.00	3.00	53.50	30.00	0.8870	0.2620
4	263.75	5.76	59.30	14.45	1.1570	0.0170
5	155.00	9.00	10.00	30.00	1.1420	0.0010
6	10.00	5.85	10.00	18.13	1.5900	0.3400
7	300.00	9.00	10.00	5.00	1.3750	0.1950
8	148.90	3.00	136.15	19.63	1.4140	0.0080
9	10.00	9.00	300.00	30.00	1.2170	0.2370
10	240.61	5.87	300.00	18.16	1.0700	0.0030
11	155.00	8.37	300.00	5.00	1.1960	0.4960
12	155.00	9.00	159.35	17.05	1.4110	0.0120
13	300.00	9.00	300.00	30.00	1.2840	0.0140
14	155.00	9.00	10.00	30.00	1.5160	0.0060
15	10.00	3.00	300.00	5.00	1.0450	0.6050
16	155.00	3.00	10.00	5.00	0.6850	0.1790
17	67.16	5.82	147.30	5.00	1.1590	0.2200
18	10.00	3.00	300.00	5.00	0.9690	0.6370
19	10.00	5.28	256.50	20.63	1.1650	0.4770
20	300.00	3.00	300.00	5.00	0.8440	0.2350
21	155.00	3.00	300.00	30.00	0.7070	0.0150
22	10.00	9.00	300.00	30.00	1.1100	0.2970
23	300.00	9.00	10.00	5.00	1.5930	0.6840
24	300.00	5.88	146.30	30.00	1.1160	0.0070
25	10.00	9.00	10.00	5.00	1.2330	0.8440

Table 3. Responses variables in photolytic degradation system of DB71

Response	Name	Units	Minimum	Maximum	Mean	Std. Dev.
Y_1	Discoloration efficiency	%	31.55	99.91	78.49	21.66
Y_2	T	°C	22.80	33.50	28.00	3.60
Y_3	pH	-	3.08	7.85	4.58	1.27
Y_4	EC	μS/cm	69.00	407.00	169.88	115.69
Y_5	TDS	mg/L	40.00	245.00	99.83	67.93

terms, respectively, and e_i is the error. Analysis of variance (ANOVA) assessed to obtain the interaction between the process variables and the responses. The quality of the fit of obtained model was expressed by the coefficient of determination R^2 and adj. R^2 in Eq. 3 and Eq.4, respectively. The statistical significance was checked with Adequate Precision (AP) ratio in Eqs. (5) and (6), and by the F-test (Adams, 2006).

$$R^2 = 1 - \frac{SS_r}{SS_m + SS_r} \tag{3}$$

$$R_{adj}^2 = 1 - \frac{SS_r / DF_r}{(SS_m + SS_r)/(DF_m + DF_r)} \tag{4}$$

$$AP = \frac{max(\hat{Y}) - min(\hat{Y})}{\sqrt{\bar{V}(\hat{Y})}} \tag{5}$$

$$\bar{V}(\hat{Y}) = \frac{1}{n}\sum_{i=1}^{n} V(\hat{Y}) = \frac{p\sigma^2}{n} \tag{6}$$

In Eq.3 and Eq. 4, SS_r and SS_m are the residual and the model sum of squares, respectively. DF denotes the degrees of freedom, p is the number of model parameters, σ^2 is the residual mean square from ANOVA table, and n is the number of experiments. AP is a signal-to-noise ratio. It compares the range of the predicted values at the design points to the average prediction error. Ratios greater than 4

indicate adequate model discrimination (Vaughn, 2007).

RESULTS & DISCUSSION

Kinetic experiments were conducted with different values of hydrogen peroxide (100 and 250 mg/L) and SiO$_2$-NP (0 and 200 mg/L). In these experiments, the initial concentration of the dye was 30 mg/L. Langmuir-Hinshelwood (L-H) model (Tang & Huren, 1995) was used to describe the relationship between the rates of the photo-catalytic degradation of dye and the dye concentration, as a function of irradiation time (Fig. 3(a)). The rate of reaction as mg/L.min is used in the form (Kumar *et al.*, 2008):

$$r = -\frac{dC}{dt} = \frac{k_r KC}{1 + KC} \tag{7}$$

where K is the adsorption coefficient of the dye on the surface of SiO$_2$-NP, k_r is the reaction rate constant, and C is the concentration at any time t. The values of kr (mg/L.min) and K (L/mg) are used to explain the effect of light intensity on the equilibrium constant for the adsorption–desorption processes between SiO$_2$-NP surface and bulk solution. By integration of Eq.7 the following equation is obtained:

$$ln\left(\frac{C_0}{C}\right) + K(C_0 - C) = k_r Kt \tag{8}$$

where C_0 is the initial concentration. For pseudo first-order reaction KC is very small as compared to 1 in the denominator of Eq. 7 so it simplified and integrated to be:

$$ln\left(\frac{C_0}{C}\right) = k_r Kt = k_1 t \tag{9}$$

The non-linearized form of first-order expression can be obtained as:

$$C = C_0 e^{-k_1 t} \tag{10}$$

where $k_1 = k_r K$ is the apparent-first-order reaction rate constant, and the half-life time $t_{1/2}$ can be calculated using the following expression:

$$t_{1/2} = \frac{0.693}{k_1} \tag{11}$$

Plotting the relation between r versus C (mg/L) and C versus irradiation time, t (min),two non-linear relationships were obtained as shown in Figs. 3(a, b), respectively. In non-linear method, the respective coefficients of determination between experimental data and the predicted values by Eq. 7 and Eq. 10 were maximized using R software and the values of k_1 constant in the first-order kinetic model and k_r and K parameters in L-H model were obtained and summarized along with half-life time in Table 4. Comparison of two models based on Adj. R^2 indicates that the oxidation kinetics of DB71 dye obey the L-H model. The rate constant of fastest reaction was 13.23 mg/L.min when the amount of H$_2$O$_2$ and SiO$_2$-NP were 250 and 200mg/L, respectively. The slowest reaction rate constant was 4.893 mg/L.min for situation when only H$_2$O$_2$was present with the concentration of 100 mg/L. The values of adsorption constants K are very low in comparison with reaction constants k_r. This shows adsorption of the dye onto the SiO$_2$-NP is not influences the photo-catalytic oxidation reaction. Therefore, the formation rate of $^{I\%}$OH will not be decreased due to decrease of the surface coverage by displacing of OH$^-$ on the SiO$_2$ surface (Tang & Huren, 1995).

(a)   (b)
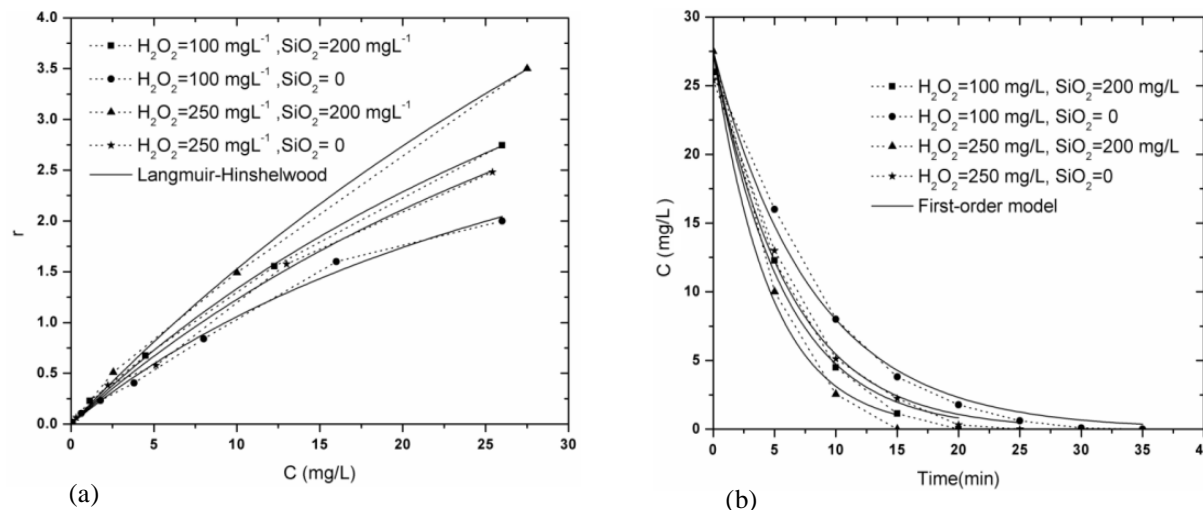
Fig. 3. Rates of DB71 degradation versus dye concentration by Langmuir-Hishelwood model (a)
First-order kinetic of DB71degradation (b)

Table 4. The rate constants and half-life time of DB71 degradation

Reactants (mg/L)	First-order model			Langmuir-Hinshelwood model		
	k_1 (min^{-1})	Adj. R^2	Half-life time (min)	k_r	K	Adj. R^2
$H_2O_2 = 100$, $SiO_2 = 200$	0.17586	0.990	3.94	8.04	0.0198	0.999
$H_2O_2 = 100$, $SiO_2 = 0.0$	0.1239	0.991	5.59	4.89	0.0275	0.995
$H_2O_2 = 250$, $SiO_2 = 200$	0.21771	0.995	3.18	13.23	0.0130	0.998
$H_2O_2 = 250$, $SiO_2 = 0.0$	0.16195	0.988	4.28	7.56	0.0194	0.995

When a photon of ultraviolet light strikes the SiO_2-NP surface, an electron from its valence band (vb) transferred to conduction band (cb) and leads to generating a positively charged hole in the valence band (h_{vb}^+). While the negative charge is increased in the conduction band (e_{cb}^-), the photo-catalytic active sites will be formed on the surface of SiO_2-NP (Sakurai, 2000) as below:

$$SiO_2 + hv \rightarrow e_{cb}^- + h_{vb}^+$$
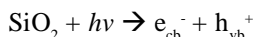
The valence band holes thus formed and react with the chemisorbed H_2O molecules to form reactive species such as $^{\bullet}OH$ radicals, which attack dye molecules successively to cause their complete degradation:

$$H_2O + h_{vb}^+ \rightarrow {^{\bullet}OH} + H^+$$

$$O_2 + e_{cb}^- \rightarrow {^{\bullet}O_2^-}$$
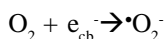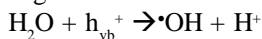
This reaction prevents the combination of the electron and the hole, which are produced in the first step. On the other side, e_{cb}^- and h_{vb}^+ can recombine on the surface of the particle within few nanoseconds and the resulting energy dissipated as heat (Badr *et al.*, 2008):

$$e_{cb}^- + h_{vb}^+ \rightarrow heat$$
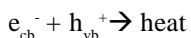
Furthermore, the e_{cb}^- and the h_{vb}^+ can be trapped in surface states where they can react with adsorbed species or close to the surface of the particle. The e_{cb}^- could react with acceptor, e.g. dissolved O_2, which consequently is transformed into super oxide radical anion ($^{\bullet}O_2^-$) leading to the additional formation of $HO_2^{\bullet}$ as given below:

$$O_2 + e_{cb}^- \rightarrow {^{\bullet}O_2^-} + (H^+ + OH^-) \rightarrow HO_2^{\bullet} + OH^-$$
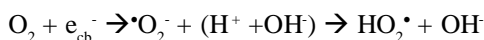
The h_{vb}^+ could also interact with donors, e.g. OH^- and $HO_2^{\bullet}$ forming $^{\bullet}OH$ radical in following manner:

$$HO_2^{\bullet} + OH^- + h_{vb}^- \rightarrow {^{\bullet}OH}$$
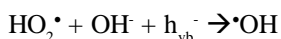
The main factor affecting the efficiency of SiO_2-NP is the amount of $^{\bullet}OH$ radicals, which can attack the DB71 molecule. H_2O_2 molecules can also absorb light energy from UV irradiation and O-O bond in its structure is ruptured leading to the production of activated $^{\bullet}OH$ and the atomic oxygen (Hu *et al.*, 2008). Increasing H_2O_2 concentration will result in an increased energy absorption and production of $^{\bullet}OH$, hence the increased oxidative destruction of DB71.

$$H_2O_2 + hv \rightarrow 2{^{\bullet}OH}$$
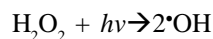
In order to keep the efficiency of the added H_2O_2, it is necessary to choose the optimum concentration of H_2O_2 according to the type and concentration of the pollutants. H_2O_2 is considered to have two functions in the photo-catalytic oxidation. It accepts a photo-generated electron from the conduction band of the semiconductor to form $^{\bullet}OH$ radical. In addition, it forms $^{\bullet}OH$ radicals according to below reactions (Kositzi *et al.*, 2004):

$$H_2O_2 + e_{cb}^- \rightarrow {^{\bullet}OH} + OH^-$$

$$H_2O_2 + {^{\bullet}O_2^-} \rightarrow {^{\bullet}OH} + OH^- + O_2$$
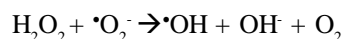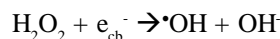
In this study photo-catalyzed oxidation kinetics of DB71 was not depends upon the change of pH. Thus, due to the lack of a significant effect of pH on the DB71 removal efficiency, this variable was not included in the approximate model proposed for DB71 removal efficiency.

The developed models equations along with the ANOVA results were presented in Table 5. The ANOVA results of the quadratic models indicated that the models Y_1, Y_2, Y_3, Y_4 and Y_5 can adequately be used to describe the dependent variables under a wide range of operating conditions. In DB71 discoloration model, adequate precision (AP) of 15.8 indicates an adequate signal. In this case, the models of the equations for the response variables are significant at 5% level. In addition, the proposed models with

Table 5. Proposed models for the response variables

Response	Equations	F Value	P value	R^2	PLOF	AP	Adj. R^2	Pred. R^2
Y_1	$37.57 + 0.34A + 1.20D - 7.84E\text{-}04A^2 - 5.16E\text{-}05C^2$	25.2	< 0.0001	0.83	0.56	15.8	0.80	0.74
Y_2	$22.58 + 0.32D$	451.5	< 0.0001	0.95	0.57	34.8	0.95	0.94
Y_3	$-5.18 + 0.0506A + 2.123B + (0.00136C) + 0.19D - (0.010AB) - 1.7E\text{-}05AC - (0.0007AD) - 0.029BD - 0.00033CD - 0.00011A^2 - (0.0653B^2) - 2.33E\text{-}05C^2 + 0.000139ABD - 2.31E\text{-}05A^2B$	60.8	< 0.0001	0.99	0.50	30.3	0.97	0.90
Y_4	$760.362 + 0.216\,A - 212.393\,B + 6.465\,D - 0.046AB + 0.010\,AD + 15.153B^2 - 0.218D^2$	87.6	< 0.0001	0.97	0.091	25.7	0.96	0.93
Y_5	$425.835 + 0.210A - 121.698B + 0.064C + 3.629D - 0.032AB + 0.0003AC + 0.006AD + 8.718B^2 - 0.125D^2$	70.9	< 0.0001	0.98	0.097	24.0	0.96	0.92

lack of fit (PLOF) more than 0.05 also reveal the lack of fit is statistically insignificant relative to the pure error.

For all models, the correlation coefficients R^2 and adjusted R^2 imply that regression models fits to the experimental data well and it can provide a good explanation of the relationships between the independent variables and the responses. The diagnostic plots of Y_1 model, shown in Fig.4, were used to estimate the adequacy of proposed model. The normal probability plot indicates whether the residuals follow a normal distribution, in which case the points will follow a straight line. The presence of a definite pattern like an "S-shaped" curve indicates that a transformation of the response may provide a better analysis. Fig. 4(a) shows that neither response transformation was needed nor there was any apparent problem with the normality. The actual and the predicted DB71 discoloration percent is shown in Fig. 4(b). In designed experiments, R^2 is a measure of the amount of reduction in the variability of the response obtained by using the independent factor variables in the model. However, a large value of R^2 does not necessarily imply that the regression model is a good one. There is a good chance that insignificant terms have been included in the model when R^2 and adj.R^2 differ dramatically (Myers *et al.*, 2009). Therefore, first should be focused on the adjusted R^2 and predicted R^2 values. A rule of thumb is that the adjusted

and predicted R^2 values should be within 0.2 of each other. For Y_1 model, the Pred. R^2 of 0.74 is in reasonable agreement with the Adj. R^2 of 0.80. APs of 34.8, 30.3, 25.7 and 24.0 for Y_2, Y_3, Y_4 and Y_5 models, respectively, indicate adequate signals. These models can also be used to navigate the design spaces. Fig. 4(c) shows the studentized residuals versus ascending predicted DB71 discoloration percent values. The general impression is that this plot should be a random, suggesting the variance of original observations to be a constant for all values of the response. Expanding variance in a megaphone-shaped pattern (<) in this plot indicates the need for a transformation (Myers *et al.*, 2009). Fig. 4(c) implies that there was no need for transformation of the discoloration percent variable. A measure of how many standard deviations the actual value deviates from the value predicted after deleting the point in question, is externally studentized residual or outlier t. Outliers should be investigated to find out if a special cause can be assigned to them. If a cause is found, then it may be acceptable to analyze the data without that point. If no special cause is identified, then the point probably should remain in the data set. Most of the standard residuals are in the range of +3.5 to -3.5 and any observation with a standardized residual outside of this interval should be considered unusual with respect to its observed response (Myers *et al.*, 2009). In Fig. 4(d), the outlier t values below the interval of ±3.50 indicated that the approximation

of the fitted model to the response surface was good. Although real wastewater is not used in this study, but to help the optimization of process, the study attempted to optimize the operating conditions of discoloration process by taking into account the effluent quality requirements. The standard suggested values for the effluent's pH, temperature, EC and TDS according to some literature were used as target values in optimization process. By numerical optimization, the value of discoloration efficiency (Y_1) was maximized while the target values of 25°C (DWAF and WRC, 1995; The American Apparel & Footwear Association (AAFA), 2010), 7.5 (Chapman, 1996) and 250 µS/cm (New South Wales *et al.*, 1995) were selected for the temperature, pH and EC respectively. The TDS was optimized in the range of 40 to 245 mg/L (New South Wales *et al.*, 1995; DWAF, 1996).

The one-factor graphs of the factors effects on the discoloration efficiency are shown in Fig. 5. As shown, the maximum discoloration is around 220 mg/

L and 155 mg/L of H_2O_2 and SiO_2-NP, respectively. Therefore, the target values of 220 and 155 mg/L were selected as goal values for H_2O_2 and SiO_2-NP respectively. The duration time of irradiation was selected as much as to provide approximately 95% discoloration (16 min). The criteria used to optimize discoloration of DB71 and the predicted values by numerical solution are shown in Table 6. The response surface graphs to investigate the interactive effect of two variables on DB71 discoloration are shown in Fig.6 (a, b, c). In the perturbation plot (Fig. 6(d)) the effects of all the factors at the optimal condition in the design space were compared. The perturbation plot helps to compare the effect of all the factors at a particular point in the design space. The response is plotted by changing only one factor over its range while holding the other factors constant. The plot was obtained for 220 mg/L H_2O_2, 155.0 mg/L SiO_2-NP, pH 9, and 16 min of reaction time. In Fig. 6 (a, b, c), the steep curvatures in SiO_2-NP and H_2O_2
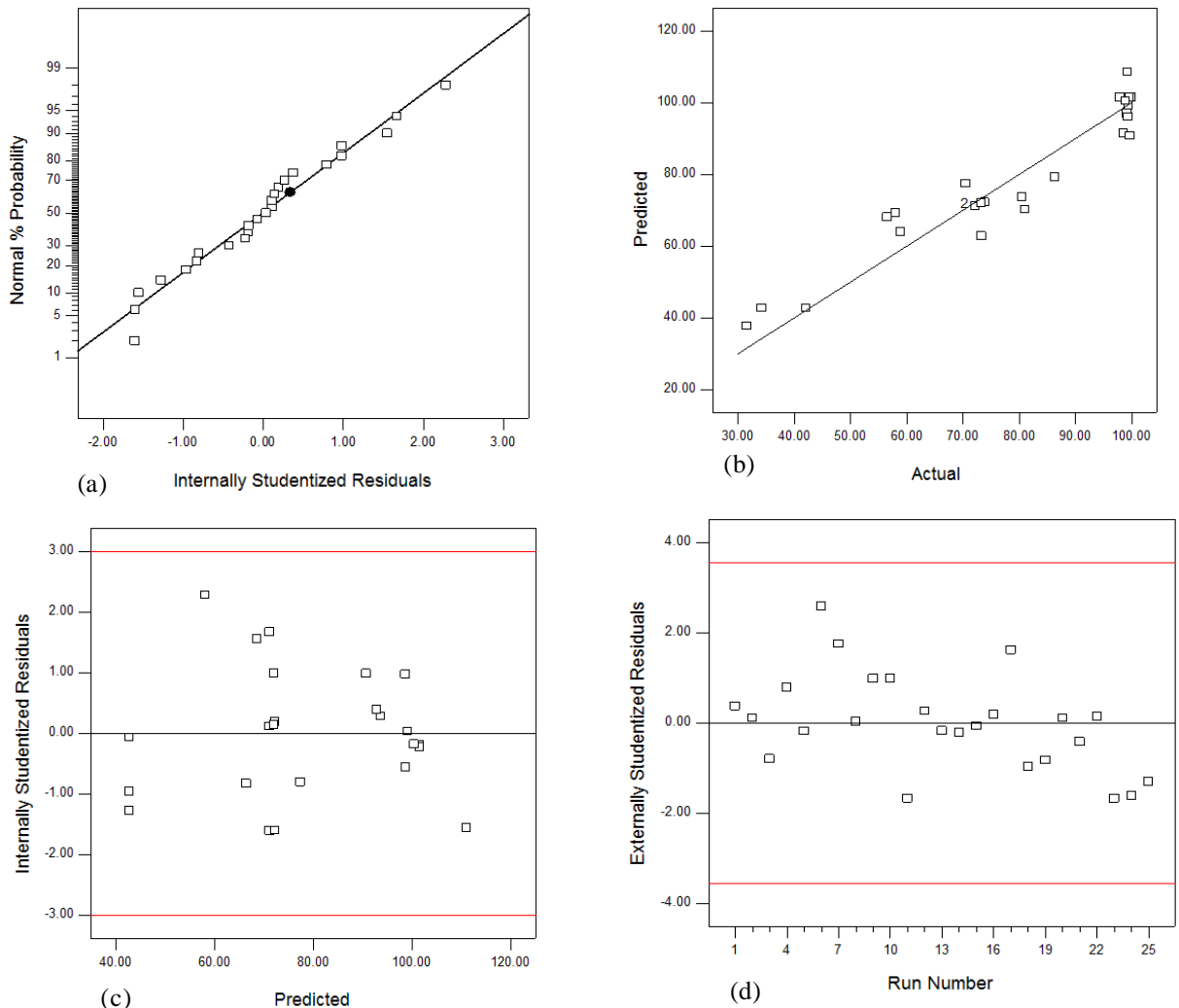
Fig. 4. Diagnostic plots of DB71 discoloration model

concentration and the linear relationship of reaction time with discoloration, show that the response of DB71 degradation is very sensitive to these three factors. In Fig. 6(a), the effect of H_2O_2 concentration on DB71 degradation is shown at pH 9. The semispherical response surface of discoloration increased with increasing H_2O_2 concentration from 20 to 220 mg/L, and then decreased slightly above

Table 6. Optimization criteria and predicted values of discoloration process

Name	Goal	Lower Limit	Upper Limit	Prediction	SE Mean	95% CI low	95% CI high
A:H_2O_2	is target = 220.0	10.0	300.0	220.0	-	-	-
B:pH	is in range	3.0	9.0	9.0	-	-	-
C:SiO_2-NP	is target = 155.0	10.0	300.0	155.0	-	-	-
D:Time	is target = 16.0	5.0	30.0	16.0	-	-	-
Discoloration (Y_1)	maximize	31.55	99.91	99.03	4.74	89.15	108.91
T (Y_2)	is target = 25	22.80	33.50	27.69	0.16	27.35	28.03
pH (Y_3)	is target = 7.5	3.08	7.85	4.54	0.17	4.16	4.93
EC (Y_4)	is target = 250	69.0	407.0	115.90	14.54	85.22	146.57
TDS (Y_5)	is in range	40.0	245.0	66.74	8.63	48.34	85.14

CI; Confidence Interval, SE; Standard Error
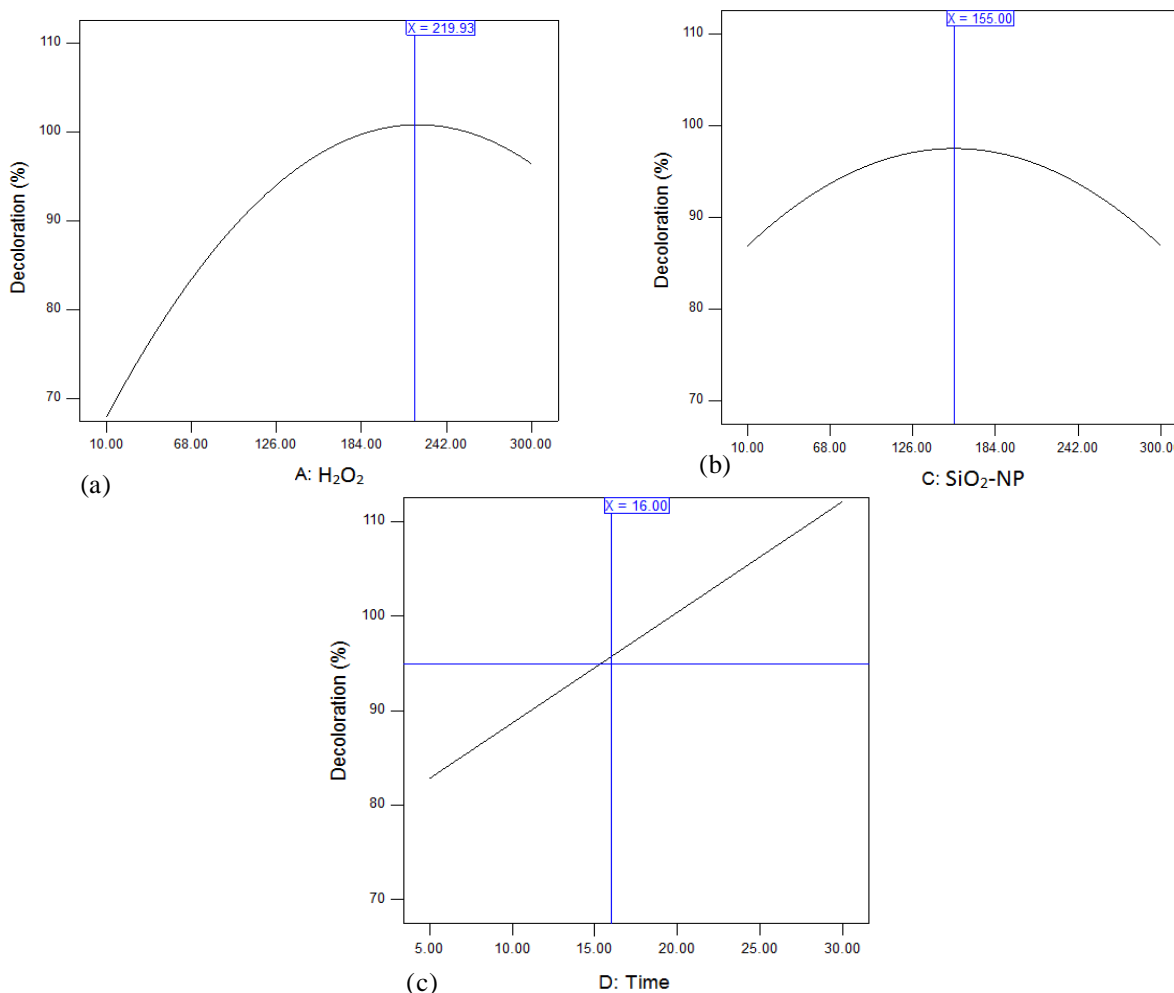
Fig. 5. One-factor graphs for the effect of H_2O_2 (a), SiO_2-NP (b) and Time (c) on DB71discoloration

(a)

(b)

(c)

(d)

Deviation from Reference Point (Coded Units)

A: H_2O_2 = 220 mg L^{-1}
*B: pH = 9
C: SiO_2-NP = 155 mg L^{-1}
D: Time = 16 min
* Factor is not in the model
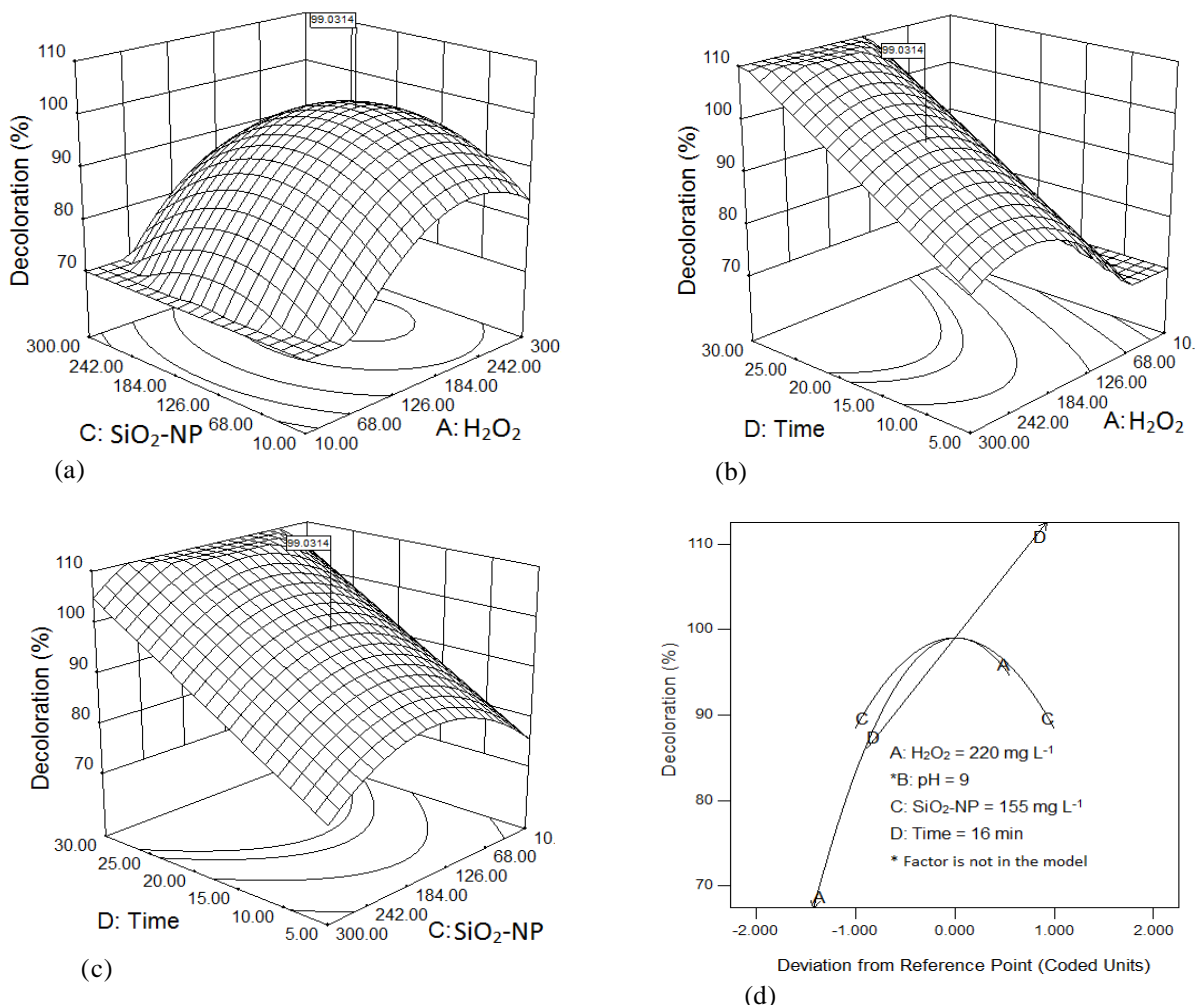
Fig. 6. The interaction effect of SiO_2-NP-H_2O_2 (a), Time-H_2O_2 (b) and Time- SiO_2-NP(c) On discoloration of DB71 and perturbation plot (d)

220 mg/L. The reason is that high concentration H_2O_2 will produce more hydroxyl radicals, which can be expected to promote DB71discoloration.

However, when H_2O_2 concentration increases over the optimum value, it can also act as the scavenger of hydroxyl radicals and causing adverse effect for dye discoloration (Zhang & Zheng, 2009).Thus, when excessive H_2O_2 is present, H_2O_2 itself becomes a significant competitor for •OH (Cater *et al.*, 2000). This may be due to the fact that excess H_2O_2 reacts with •OH and contributes to the •OH and hole scavenging to form HO_2•, H_2O and O_2 as following (Tang & Huren, 1995; Behnajady *et al.*, 2006) and leads to decease of discoloration efficiency:

•OH + H_2O_2 → H_2O + HO_2•

H_2O_2 + h_{vb}^+ → H^+ + HO_2•

HO_2• + OH →•H_2O + O_2
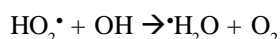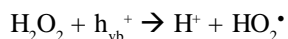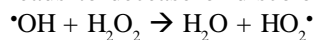
The maximum value of discoloration under optimum operating conditions was determined to be

99.03% at 16 min irradiation time. In the scope of operational and environmental considerations, the optimum values of H_2O_2 concentration and SiO_2-NP values were decided to be 220 and 155.0 mg/L, respectively. The experiment on the effect of catalyst loading showed that the increasing SiO_2-NP concentration from 10 to 155 mg/L increased the discoloration from 88.4 to 99.03% with a duration time of 16 min. With further increase of SiO_2-NP loading from 155 to 300 mg/L, the discoloration rate was decreased. This may be regards to the decrease of light penetration where light scattering effect becomes dominant (Muruganandham & Swaminathan, 2006). The optimum condition can be visualized graphically by superimposing the contours for the various response surfaces in an overlay plot (Ahmad *et al.*, 2007). Defining the optimization criteria for the chosen responses Y_1 (between 97% and 99%), Y_2 (22.8-33.5°C), Y_3 (3.07-7.85), Y_4(69-407) and Y_5 (40-245), the shaded portion of the overlay plot was generated by the Design Expert software. As shown

in Fig. 7, the optimal region corresponds to the areas, where the initial SiO_2-NP and the H_2O_2 are from 91.4 to 217.0 mg/L and 170.1 to 275.2 mg/L, respectively. To test the validity of predicted model, additional four runs were carried out under the optimum conditions obtained through RSM. The experiments were obtained as the intersection points from the overlay plot. The results of the experiments are listed in Table 7.

As sown in Table 7, the average experimental values (96.86 %) closely agreed with the theoretical predicted values of 97.03% obtained from RSM, which also confirmed that the RSM was effective and reliable for optimizing the discoloration process of DB71.

Table 7. Optimum conditions verification and additional experiments

Run	Conditions	Discoloration %	
		Actual	predicted
1	A= 222.6, C=217.0, B=9, D=16	97.54	97.09
2	A= 170.0, C=154.2, B=9, D=16	96.52	97.04
3	A= 222.6, C=91.4, B=9, D=16	95.21	96.99
4	A= 275.3, C=154.9, B=9, D=16	98.18	97.00
	Average	96.86	97.03
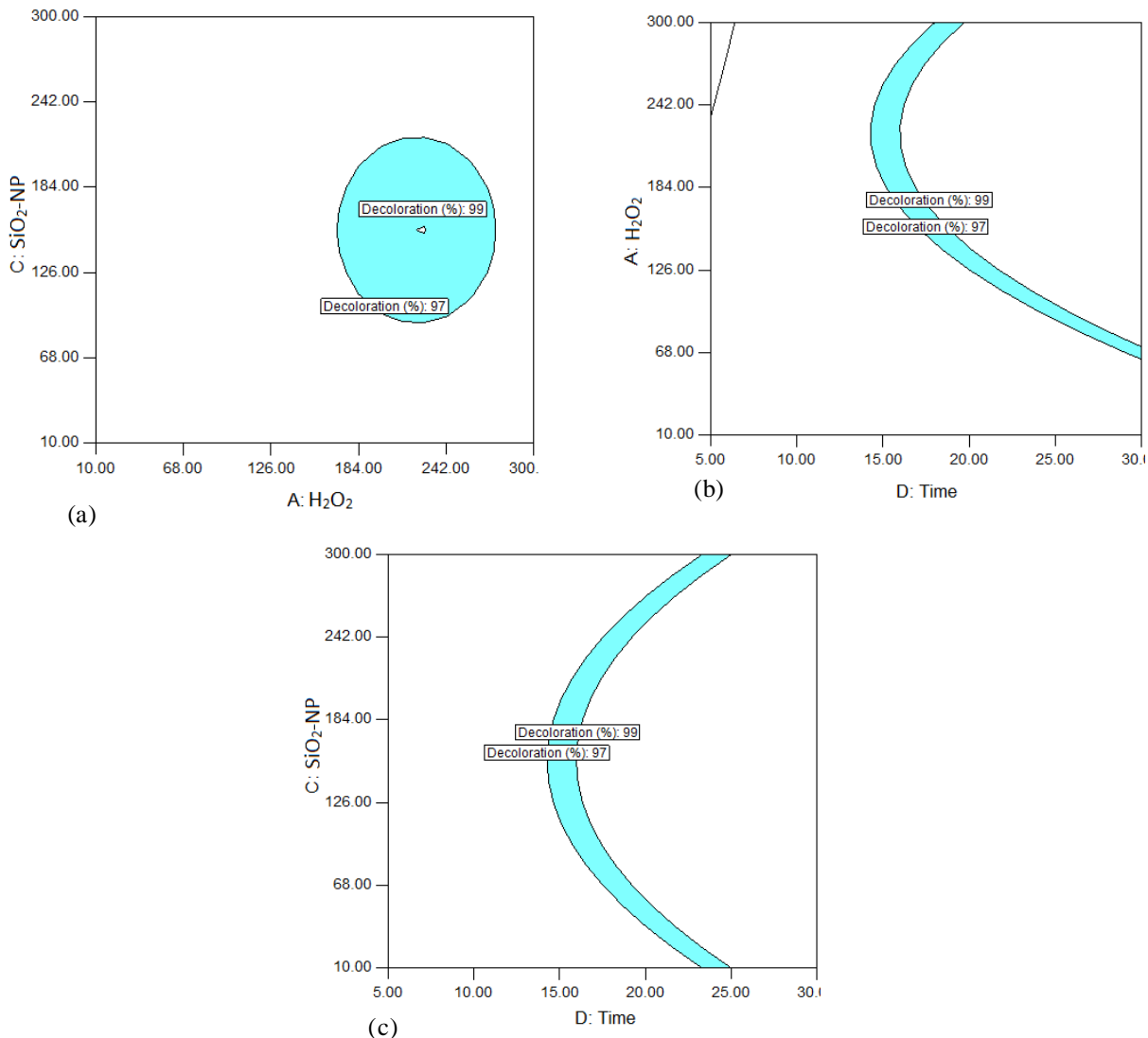
Fig. 7. Overlay plot for optimum region: SiO_2-NP versus H_2O_2 (a), H_2O_2 versus Time (b) and SiO_2-NP versus Time (c)

Table 8. Comparison of the literature results for the degradation of DB71

Dye	Performance and optimal conditions	Process	Reference
DB71	Relatively low efficiency	Sunflower Stalks as Adsorbents	(Sun & Xu, 1997)
DB71	UV/TiO2 process is more efficient compared to UV irradiation alone. Under optimal conditions (40 mg/L of catalyst, neutral pH, 45°C for 120 min irradiation) 97% removal efficiency was provided.	Circulating upflow reactor by UV/TiO_2 process	(Saien & Soleymani, 2007)
DB71	Under optimal conditions ($[H_2O_2]$ / $[Fe^{2+}]$ = 200:1, pH equal to 3.5, 45 °C for 180 min period) 99.8% efficiency was supplied	Decolorization of Direct Blue 71 from aqueous solution by Fenton process	(Tunç *et al.*, 2012)
DB71	Under optimal conditions (Fe^{2+} = 3 mg/L, H_2O_2 = 125 mg/L, pH 3.0 and 20 minutes of duration) the removal efficiency of dye was 94%.	Fenton process	(Ertugay & Acar, 2013)
DB71	Dye degradation was influenced by initial concentration and pH. In acidic pH condition the decomposition was accelerated. Combined application of UV and ZnO can increase the dye removal efficiency.	Sono, photo and sonophotocatalytic oxidation in the presence of ZnO nanocatalyst	(Ertugay & Acar, 2014)
DB71	Under optimal conditions (0.3 g/L of catalyst, pH equal to 2.5, 25°C for 25min) the removal efficiency of 100% was provided when the initial concentration was 100 mg/L of dye.	Sonocatalytic degradation of DB71 azo dye at the presence Zero-Valent Iron (ZVI)	(Ertugay & Acar, 2013)
DB71	Under the optimized condition of 155 mg/L SiO₂-NP, 220 mg/L H₂O₂ and irradiation time 16 min, discoloration was determined to be 99.03 %. discoloration increased about 11% by increasing SiO_2-NP concentration from 10 to 155 mg/L.	UV/H_2O_2 photochemical process in the presence of Nano-SiO_2 (process optimization using experimental design)	**This study**

CONCLUSIONS

The study revealed that the silica nanoparticles have some abilities to enhance the reaction rate of the dye degradation in an AOP process. In Table 8 the results of this study were compared with some other studies for the removal of DB71 from aqueous solutions.

The results showed that the discoloration increased about 11% by increasing SiO_2-NP concentration from 10 to 155 mg/L. Therefore, pure silica can accelerates the discoloration reaction rate of DB71 in the examined photo-catalytic process. The adsorption of the dye onto the SiO_2-NP was not influenced the photo-catalytic oxidation reaction. Under the optimized condition of 155 mg/L SiO_2-NP, 220 mg/L H_2O_2 and irradiation time 16 min, the experimental values agreed with the predicted ones. The maximum value of discoloration under optimum condition was determined to be 99.03 %. The reactions followed a Langmuir-Hinshelwood model. The fastest reaction rate was when the amounts of H_2O_2 and SiO_2-NP were 250 and 200 mg/L,

respectively. The slowest reaction rate was also when only H_2O_2 was present in the system.

REFERENCES

Adams, W. (2006). Handbook for Experimenters, Version 7.3, Stat-Ease, Inc., Minneapolis, MN, USA.

Ahmad, A., Wong, S., Teng, T. and Zuhairi, A. (2007). Optimization of coagulation–flocculation process for pulp and paper mill effluent by response surface methodological analysis. J. Hazard. Mat., **145 (1)**, 162-168.

Aquino, J. M., Rocha-Filho, R. C., Bocchi, N. and Biaggio, S. R. (2013). Electrochemical degradation of the Disperse Orange 29 dye on a β-PbO_2 anode assessed by the response surface methodology. J. Environ. Chem. Eng., **1 (4)**, 954-961.

Badr, Y., Abd El-Wahed, M. and Mahmoud, M. (2008). Photocatalytic degradation of methyl red dye by silica nanoparticles. J. Hazard. Mat., **154 (1)**, 245-253.

Badr, Y. and Mahmoud, M. A. (2007). Photocatalytic degradation of methyl orange by gold silver nano-core/silica nano-shell. J. Phys. Chem. Solids **68 (3)**, 413-419.

Behnajady, M. A., Modirshahla, N. and Hamzavi, R. (2006). Kinetic study on photocatalytic degradation of C.I. Acid Yellow 23 by ZnO photocatalyst. J. Hazard. Mat., **133 (1–3)**, 226-232.

Cater, S. R., Stefan, M. I., Bolton, J. R. and Safarzadeh-Amiri, A. (2000). UV/H_2O_2 treatment of methyl tert-butyl ether in contaminated waters. Environ. Sci. Technol. , **34 (4)**, 659-662.

Chapman, D. V. (1996). Water quality assessments: a guide to the use of biota, sediments, and water in environmental monitoring, World Health Organization, CRC Press.

Colpini, L. M. S., Lenzi, G. G., Urio, M. B., Kochepka, D. M. and Alves, H. J. (2014). Photodiscoloration of textile reactive dyes on Ni/TiO_2 prepared by the impregnation method: Effect of calcination temperature. J. Environ. Chem. Eng., **(In Press)**.

Cui, B., Peng, H., Xia, H., Guo, X. and Guo, H. (2013). Magnetically recoverable core–shell nanocomposites γ-$Fe_2O_3@SiO_2@TiO_2$–Ag with enhanced photocatalytic activity and antibacterial activity. Sep. Purif. Technol., **103**, 251-257.

Dong, W., Sun, Y., Ma, Q., Zhu, L., Hua, W., Lu, X., Zhuang, G., Zhang, S., Guo, Z. and Zhao, D. (2012). Excellent photocatalytic degradation activities of ordered mesoporous anatase TiO_2–SiO_2 nanocomposites to various organic contaminants. J. Hazard. Mat., **229-230**, 307-320.

DWAF (1996). South African Water Quality Guidelines, Agricultural water use irrigation. Pretoria, RSA

DWAF and WRC (1995). South African water quality management series. Procedures to Assess Effluent Discharge Impacts, Report No. TT 64/94, Department of Water Affairs and Forestry and Water Research Commission, Pretoria.

Ertugay, N. and Acar, F. N. (2013). Removal of COD and color from Direct Blue 71 azo dye wastewater by Fenton's oxidation: Kinetic study. Arabian Journal of Chemistry, **(In Press)**.

Ertugay, N. and Acar, F. N. (2013). Sonocatalytic degradation of Direct Blue 71 azo dye at the presence Zero-Valent Iron (ZVI). Desalination and Water Treatment, **51 (40-42)**, 7570-7576.

Ertugay, N. and Acar, F. N. (2014). The degradation of Direct Blue 71 by sono, photo and sonophotocatalytic oxidation in the presence of ZnO nanocatalyst. Applied Surface Science, **(In Press)**.

Fernades Rêgo, F. E., Sales Solano, A. M., da Costa Soares, I. C., da Silva, D. R., Martinez Huitle, C. A. and Panizza, M. (2014). Application of electro-Fenton process as alternative for degradation of Novacron Blue dye. J. Environ. Chem. Eng., **2 (2)**, 875-880.

Fornasari, G. and Trifirò, F. (1998). Oxidation with no-redox oxides: ammoximation of cyclohexanone on amorphous silicas. Catal. Today, **41 (4)**, 443-455.

Fraga, L. E., Franco, J. H., Orlandi, M. O. and Zanoni, M. V. B. (2013). Photoelectrocatalytic oxidation of hair dye basic red 51 at $W/WO_3/TiO_2$ bicomposite photoanode activated by ultraviolet and visible radiation. J. Environ. Chem. Eng., **1 (3)**, 194-199.

Hadi, M., McKay, G., Samarghandi, M. R., Maleki, A. and Solaimany Aminabad, M. (2012). Prediction of optimum adsorption isotherm: comparison of chi-square and Log-likelihood statistics. Desalination and Water Treatment, **49 (1-3)**, 81-94.

Hadi, M., Samarghandi, M. R. and McKay, G. (2011). Simplified fixed bed design models for the adsorption of acid dyes on novel pine cone derived activated carbon. Water, Air, Soil Pollut. , **218 (1)**, 197-212.

Hu, Q., Zhang, C., Wang, Z., Chen, Y., Mao, K., Zhang, X., Xiong, Y. and Zhu, M. (2008). Photodegradation of methyl tert-butyl ether (MTBE) by UV/H_2O_2 and UV/TiO_2. J. Hazard. Mat., **154 (1-3)**, 795-803.

Ibrahim, D. S., Praveen Anand, A., Muthukrishnaraj, A., Thilakavathi, R. and Balasubramanian, N. (2013). In situ electro-catalytic treatment of a Reactive Golden Yellow HER synthetic dye effluent. J. Environ. Chem. Eng., **1 (1–2)**, 2-8.

Kositzi, M., Antoniadis, A., Poulios, I., Kiridis, I. and Malato, S. (2004). Solar photocatalytic treatment of simulated dyestuff effluents. Solar Energy, **77 (5)**, 591-600.

Kumar, K. V., Porkodi, K. and Rocha, F. (2008). Langmuir–Hinshelwood kinetics – A theoretical study. Catal. Commun., **9 (1)**, 82-84.

Kumar, S. and Singh, R. K. (2014). Optimization of process parameters by response surface methodology (RSM) for catalytic pyrolysis of waste high-density polyethylene to liquid fuel. J. Environ. Chem. Eng., **2 (1)**, 115-122.

McKay, G., Hadi, M., Samadi, M. T., Rahmani, A. R., Aminabad, M. S. and Nazemi, F. (2011). Adsorption of reactive dye from aqueous solutions by compost. Desalination and Water Treatment, **28 (1-3)**, 164-173.

McKay, G., Mesdaghinia, A., Nasseri, S., Hadi, M. and Solaimany Aminabad, M. (2014). Optimum isotherms of dyes sorption by activated carbon: Fractional theoretical capacity & error analysis. Chemical Engineering Journal, **251**, 236-247.

Megouda, N., Cofininier, Y., Szunerits, S., Hadjersi, T., ElKechai, O. and Boukherroub, R. (2011). Photocatalytic activity of silicon nanowires under UV and visible light irradiation. Chem. Commun., **47 (3)**, 991-993.

Muruganandham, M. and Swaminathan, M. (2006). Advanced oxidative decolourisation of Reactive Yellow 14 azo dye by UV/TiO_2, UV/H_2O_2, $UV/H_2O_2/Fe^{2+}$ processes - a comparative study. Sep. Purif. Technol., **48 (3)**, 297-303.

Myers, R. H., Montgomery, D. C. and Anderson-Cook, C. M. (2009). Response surface methodology: process and product optimization using designed experiments, Vol. 705, John Wiley & Sons.

New South Wales, Environment Protection Authority and Waters and Catchments Branch (1995). The Utilisation of

treated effluent by irrigation : draft environmental guidelines for industry / Waters and Catchments Branch, Environment Protection Authority Bankstown, N.S.W.

Saien, J. and Soleymani, A. R. (2007). Degradation and mineralization of Direct Blue 71 in a circulating upflow reactor by UV/TiO2 process and employing a new method in kinetic study. Journal of Hazardous Materials, **144 (1–2)**, 506-512.

Saitoh, T., Saitoh, M., Hattori, C. and Hiraide, M. (2014). Rapid removal of cationic dyes from water by coprecipitation with aluminum hydroxide and sodium dodecyl sulfate. J. Environ. Chem. Eng., **2 (1)**, 752-758.

Sakurai, Y. (2000). The 3.1 eV photoluminescence band in oxygen-deficient silica glass. J. Non-Cryst. Solids, **271 (3)**, 218-223.

Satapathy, M. K. and Das, P. (2014). Optimization of crystal violet dye removal using novel soil-silver nanocomposite as nanoadsorbent using response surface methodology. J. Environ. Chem. Eng., **2 (1)**, 708-714.

Shen, Z.-Y., Li, L.-Y., Li, Y. and Wang, C.-C. (2011). Fabrication of hydroxyl group modified monodispersed hybrid silica particles and the h-SiO_2/TiO_2 core/shell microspheres as high performance photocatalyst for dye degradation. J. Colloid Interface Sci., **354 (1)**, 196-201.

Skuja, L. (2000). Optical properties of defects in silica. (In G. Pacchioni, S. Linards and L. G. David (Eds.),Defects in SiO_2 and related dielectrics: Science and technology (pp. 73-116). Springer)

Sun, G. and Xu, X. (1997). Sunflower Stalks as Adsorbents for Color Removal from Textile Wastewater. Industrial & Engineering Chemistry Research, **36 (3)**, 808-812.

Taha, M., Adetutu, E. M., Shahsavari, E., Smith, A. T. and Ball, A. S. (2014). Azo and anthraquinone dye mixture decolourization at elevated temperature and concentration by a newly isolated thermophilic fungus, Thermomucor indicae-seudaticae. J. Environ. Chem. Eng., **2 (1)**, 415-423.

Tang, W. Z. and Huren, A. (1995). UV/TiO_2 photocatalytic oxidation of commercial dyes in aqueous solutions. Chemosphere, **31 (9)**, 4157-4170.

The American Apparel & Footwear Association (AAFA) (2010). Global Textile Effluent Guidelines.

Tolia, J., Chakraborty, M. and Murthy, Z. (2012). Photocatalytic degradation of malachite green dye using doped and undoped ZnS nanoparticles. Pol. J. Chem. Technol., **14 (2)**, 16-21.

Tunç, S., Gürkan, T. and Duman, O. (2012). On-line spectrophotometric method for the determination of optimum operation parameters on the decolorization of Acid Red 66 and Direct Blue 71 from aqueous solution by Fenton process. Chemical Engineering Journal, **181–182**, 431-442.

Vaughn, N. (2007). Design-Expert® software. Stat-Ease, Inc, Minneapolis, MN.

Yu, S., Chen, Z., Cheng, Q., Lü, Z., Liu, M. and Gao, C. (2012). Application of thin-film composite hollow fiber membrane to submerged nanofiltration of anionic dye aqueous solutions. Sep. Purif. Technol., **88**, 121-129.

Zhai, J., Tao, X., Pu, Y., Zeng, X.-F. and Chen, J.-F. (2010). Core/shell structured ZnO/SiO_2 nanoparticles: Preparation, characterization and photocatalytic property. Appl. Surf. Sci., **257 (2)**, 393-397.

Zhang, D. (2012). Heterogeneous photocatalytic removal and reaction kinetics of Rhodamine-B dye with Au loaded TiO_2 nanohybrid catalysts. Pol. J. Chem. Technol., **14 (2)**, 42-48.

Zhang, Z. and Zheng, H. (2009). Optimization for decolorization of azo dye acid green 20 by ultrasound and H_2O_2 using response surface methodology. J. Hazard. Mat., **172 (2)**, 1388-1393.

Zodi, S., Merzouk, B., Potier, O., Lapicque, F. and Leclerc, J.-P. (2013). Direct Red 81 dye removal by a continuous flow electrocoagulation/flotation reactor. Sep. Purif. Technol., **108**, 215-222.